Aquat.sci.63 (2001) 250–264
1015-1621/01/030250-15 $ 1.50+0.20/0


Aquatic Sciences

# Incident and *in situ* irradiance in Lakes Cadagno and Lucerne: A comparison of methods and models

Patrick J. Neale[1,*], Peter Bossard[2], Yannick Huot[3], and Ruben Sommaruga[4]

[1] Smithsonian Environmental Research Center, Edgewater, MD USA
[2] Limnological Research Center, EAWAG, CH-6047 Kastanienbaum, Switzerland
[3] CEOTR, Dept. of Oceanography, Dalhousie University Halifax, Nova-Scotia B3H 4J1, Canada
[4] Institute of Zoology and Limnology, University of Innsbruck, Technikerstrasse 25, A-6020 Innsbruck, Austria

*Key words:* Lake Lucerne, Lake Cadagno, PAR, UV-A, UV-B, irradiance regime, radiative transfer models, altitude effect.

ABSTRACT

Incident surface irradiance of photosynthetically available radiation (PAR), and ultraviolet radiation (UV-A and UV-B) was monitored during the GAP Workshop (8–15 September 1999) at the field stations Kastanienbaum at Lake Lucerne (434 m a.s.l.) and Piora at Lake Cadagno (1923 m a.s.l.), Switzerland, with broad band sensors (LiCOR and Macam) and multifilter spectral radiometers (Smithsonian UV-B radiometer SR18, Satlantic and Biospherical Profilers). Calculations of clear sky spectral irradiance were performed using computer implementations of atmospheric radiative transfer models STAR and FASTRT as well as a simple two-stream model. Clear sky conditions prevailed at Lucerne so that detailed comparisons could be made between measured irradiance and model predictions. Good correspondence was found for the measurements and predictions. The best agreement was with the STAR model. Spectral measurements were consistent with measurements of the broad band UV-A and UV-B sensors after accounting for the manufacturer specified spectral response. The effective center wavelength of the broad band UV-B sensor is 320 nm, despite the fact that the maximum sensitivity of the sensor is at 310 nm. A daily UV index was estimated from the midday SR18 data. An analysis of the UV-A and UV-B data at the two sites of different altitude indicates that the so called altitude effect (AE) is variable during the course of the day and usually higher for UV-B than for UV-A. Lakes Lucerne and Cadagno have moderate transparency to UV and PAR with 50 % of 320 nm irradiance penetrating to 1 m in Lake Lucerne and 0.3 m in Lake Cadagno.

## Introduction

Absorption and scattering processes in the atmosphere are wavelength dependent. For that reason, variations in solar elevation, cloudiness, relative humidity, atmospheric turbidity and ozone will affect the photosynthetically available radiation (PAR), and ultraviolet radiation (UV-A and UV-B) components of the incident

* Corresponding author, e-mail: Neale@serc.si.edu

solar radiation at the surface to different extents. Below the surface in the aquatic environment, the water, and the dissolved and particulate components it contains, affect the wavelength-specific transmission of light with depth. All these factors have to be taken into account when spectral irradiance models are used. Moreover, by varying the spectral profile of incident irradiance, these processes complicate the measurement and interpretation of irradiance measurements, especially those made with broad band sensors. This becomes particularly crucial when weightings are applied to the irradiance.

During the GAP workshop, to explore the effects of these processes on primary productivity and ultraviolet inhibition, measurements of incident irradiance were performed with a variety of radiometric instruments over the shortwave spectrum, including the UV (290–400 nm) and PAR (400–700 nm) bands. The main goal was to specify the underwater irradiance regime, the primary forcing variable for aquatic primary production. Secondary goals were (i) to compare irradiance measurements between instruments and between sites, and (ii) to obtain information on the so called "altitude effect" of incident surface irradiance. Instrumentation was provided by workshop participants and was also supported by routine monitoring data from the Swiss Meteorological Agency (SMA).

## Methods

*Broadband sensors:* Downwelling PAR, UV-A and UV-B were continuously monitored at the field stations Kastanienbaum and Piora within 3 km of the sampling sites (see Bossard et al., Fig. 1), using cosine corrected sensor for PAR (LI 190, LI-COR) and UV (SD 104/UV-A and SD 104/UV-B, Macam), and an integrator (LI 1000, LI-COR). The UV-A sensor has a high sensitivity in a narrow peak at 370 nm ±10 nm and covers a bandwidth of ca. 80 nm (from 320–400 nm), the UV-B sensor peaks at 310 nm ± 10 nm and covers a band width of ca. 80 nm (from 280–360 nm) (Fig. 1). The integrator was set to measure and record the averages

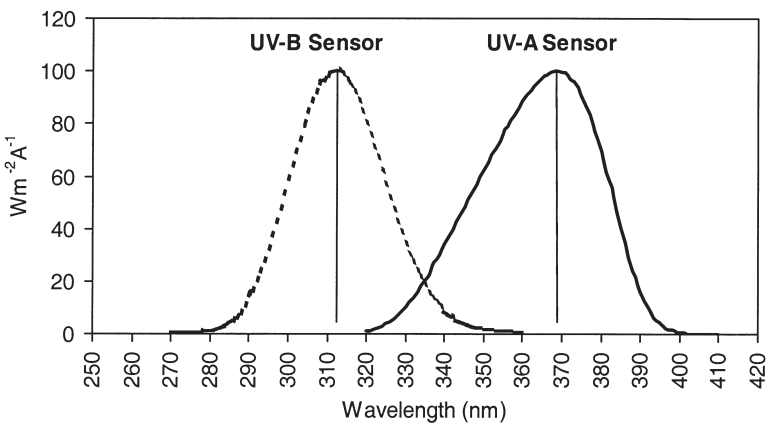


**Figure 1.** Spectral response of the Macam UV sensors SD 104/UV-A and SD 104/UV-B

of the continuous output of PAR, UV-A and UV-B for each 10 min interval of the day.

The PAR, UV-A and UV-B sensors used at Kastanienbaum (monitoring set, always set up) and Piora (installed for GAP) were cross calibrated in simultaneous field measurements on July 13–16, 1999, at Kastanienbaum, to adjust the logger coefficients, before using them for this study. Another set of the same sensors was used for the assessment of underwater irradiance depth profiles (for details, see Bossard et al., 2001, this issue).

*Smithsonian UV-B radiometer:* This instrument was designed and constructed by the Photobiology/Solar Radiation laboratory of the Smithsonian Environmental Research Center (SERC). The radiometer sensor head unit is a weather proof housing with a cosine-corrected diffuser to measure planar downwelling irradiance, an interference filter wheel with 18 interference filters mounted in the periphery, a collimator, and a solar blind R-1657 photomultiplier tube. The photomultiplier tube (PMT) housing is temperature regulated (25 °C) with a thermostated thermopeltic system. The filter wheel turns at 15 rpm and the filters have a bandpass (FWHM) of 2 nm and nominal center wavelengths at 2 nm intervals from 290 to 324 nm. The PMT current output is converted to voltage and is filtered for electronic noise, amplified, and passed to a precision monolithic 20 bit A/D converter. Operation of the system is under the control of a microcontroller. Data from all channels, two dark readings and internal temperature are averaged for one minute intervals, stored along with control information, then transmitted over an RS-232 twisted pair modem to a data acquisition computer. All components of the sensor head, except the PMT, are designed to operate without significant temperature effects from −25° to +70 °C. Further information on instrument performance is provided in (Thompson et al., 1997; Early et al., 1998).

During the GAP-Workshop, an SR-18 instrument (serial number UN) was located on the roof of the EAWAG laboratory for the period of 8 through 14 September, 1999. Measurements were made near Lake Cadagno (Piora) on 15 September, 1999. Calculated spectral irradiance was based on the average of calibrations made using a 1000 W NIST-traceable lamp at SERC before and after the deployment period.

*Satlantic Lake Profiling Radiometer:* The instrument is an OCI-200 head connected to a STORDAT acquisition and storage system. The instrument has the following channels: 304.9, 323.4, 338.2, 380.5, 443.2, 490.6, 554.5 nm. The 304.9 channel was not functional during the GAP workshop. The instrument is self logging and battery operated. It has a depth sensor and a temperature sensor for profiling. The cosine collectors are optimized for in water use. For the assessment of surface irradiance the instrument was positioned on a hill about 200 meters away from lake Cadagno.

*Biospherical Profiling Radiometer:* A Biospherical Instruments PUV-500 was used to measure profiles of downwelling PAR and UV. The UV is measured in four channels with nominal 10 nm bandwidth in the UV with typical center band wavelengths of 305, 320, 340 and 380 nm. It also has a depth sensor. Data is logged through a cable to a surface data acquisition computer.

*Calculation of underwater vertical attenuation coefficients:* The attenuation coefficient, $K_d$ [$m^{-1}$], describes the vertical gradient in underwater irradiance according to Beer's law, i.e. $E_z(\lambda) = E_0(\lambda) \cdot \exp(-K_d(\lambda) \cdot z)$, where $E_z(\lambda)$ is irradiance at depth $z$ (0 = surface). The depth profile of $K_d$ was calculated as the slope of logarithm of the irradiance over each depth interval. This was calculated every 10 cm through the water column using a depth interval of 50 cm. From this profile, layers of approximately homogeneous optical properties were defined. An overall $K_d$ for these layers was fitted as the slope of the linear regression of $\ln(E_z)$ vs. depth.

*Radiative Transfer Models:* Calculations of clear sky spectral irradiance were performed using two computer implementations of atmospheric radiative transfer models selected because programs are publicly available. The System for Transfer of Atmospheric Radiation (STAR) package uses matrix operator theory (Ruggaber et al., 1994) and was developed by Dr. Harry Schwander at the Meteorological Institute of the University of Munich who makes available a computer package for running the model under Windows 95/98. The FASTRT package is based on the SDISORT model of (Dahlback and Stamnes, 1991) and is implemented via a web-interface at the Norut Information Technology institute in Tromsø, Norway (www.itek.norut.no/~olae/fastrt). Calculations of spectral irradiance were also performed with the simple two-stream model of Gregg and Carder (1990) as modified by Arrigo (1994) using a MATLAB implementation (cf. Neale et al. 1998). Input data for the models were time, geographic position, TOMS total column ozone, barometric pressure and altitude. A 1 nm bandwidth was specified. Additionally, in the STAR package a "summer" ozone profile and "continental" aerosol were selected. Default values were used for all other parameters.

## Results

### *Weather conditions and surface irradiance*

Clear, albeit hazy, conditions prevailed during the entire workshop period presenting an excellent opportunity for comparative radiometry. Figure 2 shows the daily time courses of surface irradiance (PAR, UV-A and UV-B) at the Alpine Biological Station at Piora (Lake Cadagno) and at the Limnological Research Center at Kastanienbaum (Lake Lucerne) during the GAP Workshop. While at Kastanienbaum clouds were absent during the whole period from 12 to 15 September, scattered clouds were present after midday at Piora on the 12, 14, and 15 September as is common for high altitude sites.

### *UV exposure*

As a general indicator of the amount of biologically effective UV during the period, a daily UV index was estimated from the midday SR18 data. The UV index is the mean weighted UV for erythema (mW $m^{-2}$) during the 1 hour period centered around solar noon (12:00 h in CET*) divided by 25 (Long et al., 1996). The UV index

* CET (= GMT+1) time zone is used in this paper. CEST (summer time, i.e. local during workshop, = GMT+2) is used in other papers in this issue.

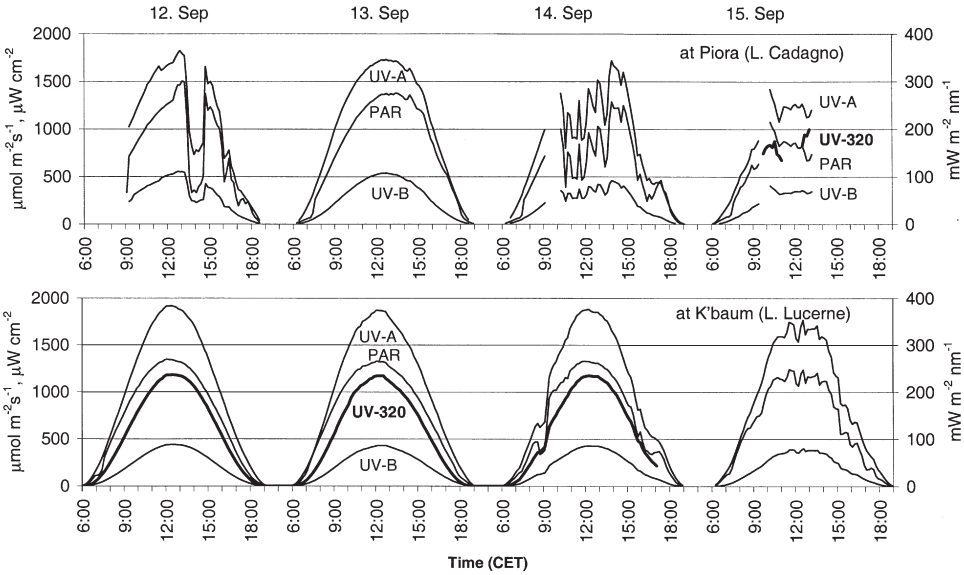


**Figure 2.** Time course of surface irradiance ($E_o$) at Piora (L. Cadagno) and at Kastanienbaum (L. Lucerne) during the GAP Workshop (12–15 Sept. 1999): PAR (µmol $m^{-2}$ $s^{-1}$), UV-A, UV-B (µW $cm^{-2}$) and UV at 320 nm (mW $m^{-2}$ $nm^{-1}$). All values are 10 minute averages

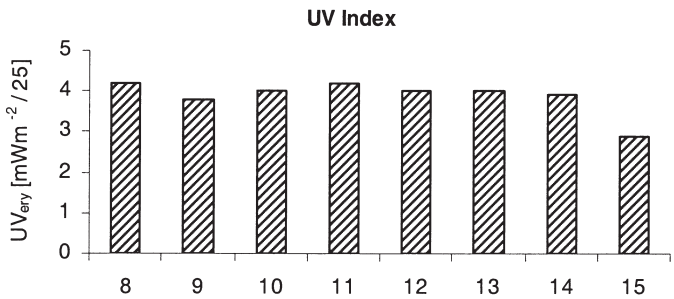


**Figure 3.** UV Index at Kastanienbaum (L. Lucerne, 8–14) and Piora (15) during the GAP Workshop (8 – 15 September)

at Lucerne (Fig. 3) varied between 3.9 to 4.2 (average 4.0 $UV_{ery}$ [mW $m^{-2}$/25]) indicating a moderate exposure hazard for sunburn (10 is the typical maximum UV index value for the temperate zone near sea level).

*Comparisons of observed and modeled spectral irradiance*

The SR18 measurements and model output were compared for midday, clear sky conditions on 14 September (Fig. 4). In general, there was close correspondence between the SR18 measurements and the STAR model calculations. The two only

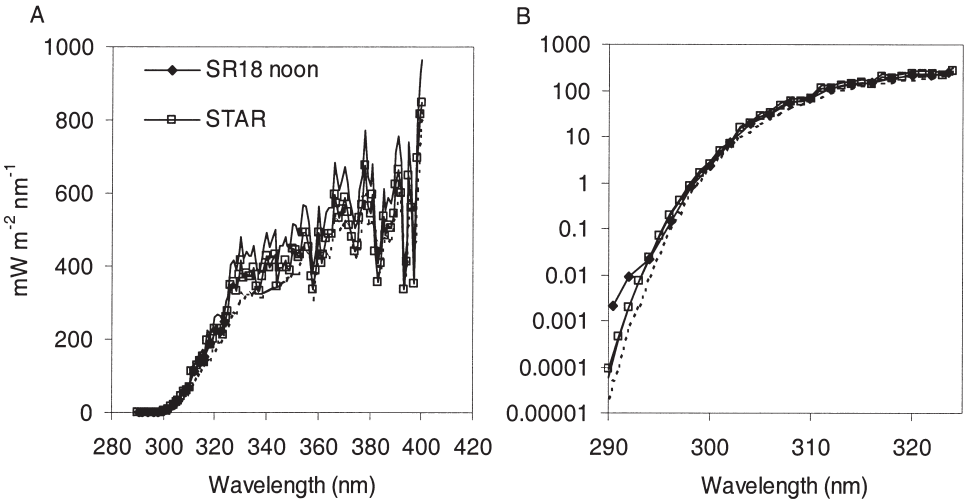


**Figure 4.** Comparison of midday solar spectral irradiance(mW $m^{-2}$ $nm^{-1}$), 14 September 1999, as measured by the SR18 UV-B spectroradiometer (solid line, open symbols), and as calculated by radiative transfer models implemented by the STAR program (solid line, solid symbols), FASTRT program (solid line) and a two-stream model (Gregg and Carder, 1990) (broken line). (A) full UV spectrum on linear irradiance scale, (B) UV-B spectrum on a logarithmic scale

diverged at the shortest wavelengths measured by the SR18 (290 and 292 nm), for which the 2 nm bandwidth of the SR18 probably results in an effective shift in the center wavelength of the filter (see Correll et al., 1992). The FASTRT model produced values that were generally about 20% higher than the SR18. The Gregg and Carder model calculations, on the other hand, was consistently lower than the SR18. Based on this comparison, the STAR model was selected for further evaluation.

Model performance over the course of a day was evaluated for Kastanienbaum for 13 September, 1999 which was clear all day. Model irradiance was calculated between 06:30 h and 17:00 h (Central European Time = GMT + 1) at a 0.5 h intervals (Fig. 5). Again, there was close correspondence between the model and measurements of the SR18, for example; the time course of 320 nm irradiance is shown in Fig. 5-A. To further evaluate the model output, the relative spectral response function of the Macam UV-B and UV-A sensors (provided by the manufacturer) was applied to the STAR generated spectra. Agreement between the model and the broadband observations was comparable to the agreement between the model and the SR18 at 320 nm (Fig. 5-B, C). Model irradiance was also converted to quantum flux using the conversion

$$Q(\lambda) = \frac{E(\lambda) \cdot \lambda}{119.67} \quad (1)$$

where $Q$ is quantum flux in μmol $m^{-2}$ $s^{-1}$ $nm^{-1}$, $E$ is irradiance in W $m^{-2}$ $nm^{-1}$, and $\lambda$ is wavelength in nm. Quantum flux was integrated between 400 and 700 nm for com-

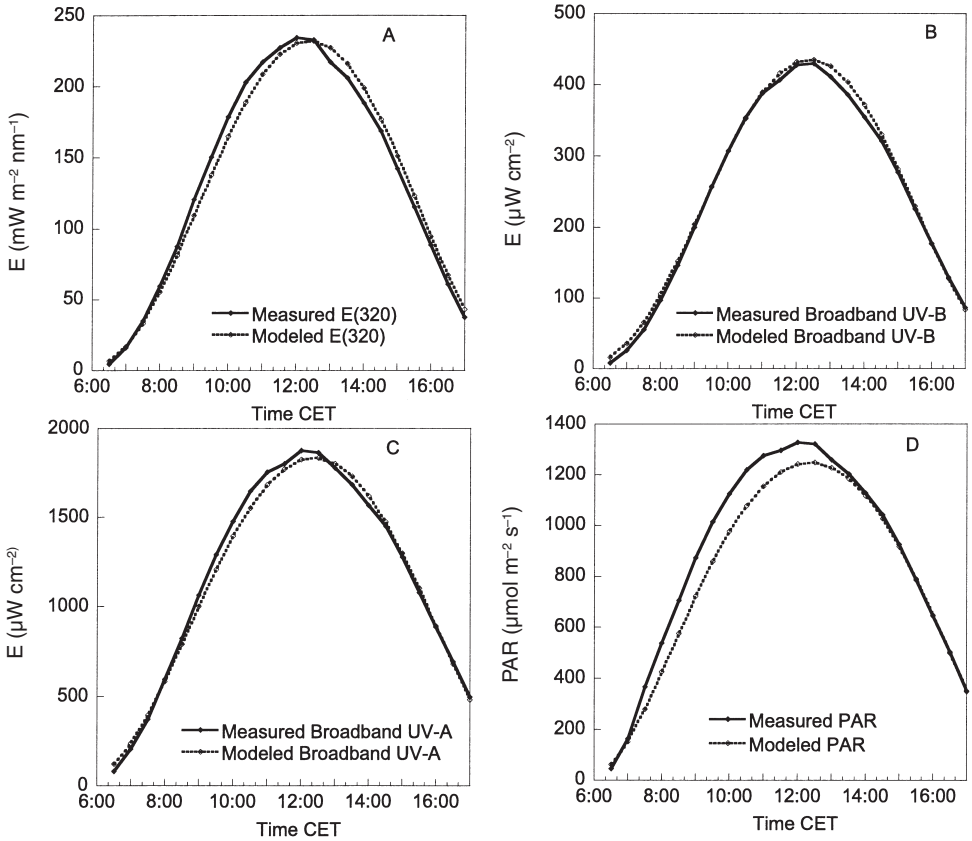


**Figure 5.** Variation of irradiance with time of day for 13 September at the EAWAG laboratory in Kastanienbaum, comparing calculations using the STAR radiative transfer model (solid line, closed symbols) and radiometer measurements (dashed line, open symbols) of (A) irradiance at 320 nm measured by the SR18 UV-B spectroradiometer, irradiance measured by a Macam SD104/UV-B (B) and UV-A (C) sensors (sensor spectral response was applied to modeled spectral irradiance for comparison) (D) incident photon flux of PAR (Licor LI-192)

parison with measured quantum flux of PAR (Fig. 5-D). The model underestimated measured PAR during midday, but was very close to the measured value for the afternoon period. These results suggested that the STAR model under these conditions provides accurate solar spectral irradiance data, and, in particular, can be used as input data to evaluate the underwater spectral irradiance for the UV-A and PAR irradiance for the cases when only broadband measurements were made during the workshop (these results are used in other analyses of UV effects presented in Bossard et al., 2001; Callieri et al., 2001; Köhler et al., 2001; and Neale et al., 2001; all in this issue).

*Instrument comparison*

Three different types of instruments made measurements of incident UV during the workshop, the SR-18 (290–324 nm), the Satlantic STOR-DAT (305, 323, 338, and 380 nm) and the Macam broadband UV-A and UV-B sensors. The SR-18 and the Satlantic share a common wavelength near 323 nm, so could be directly compared. The comparison was performed on the morning of 15 September at Piora. Usable data was obtained from both instruments over the period 10:00 h to 12:00 h (CET, 1 min intervals). Comparison of the 323 nm irradiance (mW $m^{-2}$ $nm^{-1}$) measurements showed a good linear relationship, though intermittent cloudiness caused some scatter ($R^2 = 0.92$). The scatter was probably due to the differing time response of each instrument. On an absolute basis, the SR18 measurement was 71 % of the STOR-DAT reading. The STOR-DAT collector is optimized for underwater collection, so the difference may be caused by a deviation from a true cosine response during in air measurements using the OCI-200 optical head. Alternatively, slightly different wavebands could account for the difference.

Absolute comparisons of the spectral and broadband instruments requires the application of the spectral response function of the broadband instruments to spectral irradiance. Even though direct spectral irradiance measurements were not made in the UV-A, we were able to apply the spectral response function to model output which was validated by comparison with the SR-18 in the UV-B (Fig. 5). These results suggest that the UV-A and UV-B sensors at Kastanienbaum were performing according to manufacturer's specification. Similar data was also obtained at Piora, but the UV-A sensor was operating correctly only on 14 and 15 September. This limited data was consistent with the UV-A and UV-B sensors at Piora also performing according to the manufacturer's specification.

Another absolute comparison was performed on 15 September with the Macam UV-B sensor at Piora. But the available data was limited by short period of SR18 operation. On other days, model spectra were generated but intermittent cloudiness limited the number of clear-sky broadband measurements. The limited results available, however, indicated a near 1:1 correspondence between observed and predicted broadband response for the Piora UV-B sensor.

An alternative to an absolute comparison is to find the wavelength at which the broadband sensor has the strongest correlation with spectral irradiance. This is termed the effective center wavelength of the broadband measurement. To accomplish this, correlations were performed between the Kastanienbaum Macam UV-B sensor and the each of the 18 channels of the SR-18 over a whole day. The Macam UV-B sensor reading displayed good linear correlations (no curvature in the relationship over the whole day) with SR18 data for each channel from 316 to 322 nm. The best agreement was at 320 nm, with the SR18 measurement ($E(320)$, mW $m^{-2}$ $nm^{-1}$) = 0.51 × Macam Kastanienbaum UV-B (μW $cm^{-2}$) ($R^2 = 0.99$). Since a full day of SR18 irradiance observations were not available for Piora, a two step comparison was made. On 12 September, the Satlantic and the Piora Macam UV-B sensor were functioning for the full day. A good relationship was obtained between the two measurements, after smoothing the Satlantic data as appropriate for the 10 minute averaging period of the Macam sensor data logger. It was found that the Satlantic $E(323)$ (mW $m^{-2}$ $nm^{-1}$) = 0.72 × Macam Piora UV-B (μW $cm^{-2}$) ($R^2 = 0.99$). Com-

bining this relationship with the comparison of the Satlantic and SR18 on 15 September [for which SR18 $E(320) = 0.65 \times$ Satlantic $E(323)$, $R^2 = 0.93$], we obtained an overall relationship SR18 $E(320) = 0.47 \times$ Macam Piora UV-B ($\mu W\ cm^{-2}$). As an independent check, we also compared model output at 320 nm for Piora and the Macam sensor UV-B for nine clear sky observations over the day on September 12, and obtained a similar relationship (coefficient of 0.47). We conclude that the UV-B sensors at Piora and Kastanienbaum performed with similar spectral response and absolute sensitivity.

*These observations lead to the following conclusions concerning the comparison of instruments and of observed and modeled irradiance:*

1. The workshop provided a good setting to compare various approaches to estimating solar irradiance including different types of instruments and numerical models.
2. The STAR program calculated irradiances that were quite close to those measured under clear sky conditions. The FASTRT program tended to overestimate irradiance. The STAR and FASTRT programs are both radiative transfer models and most radiative transfer models give similar results when identical input data and boundary conditions are provided (Koepke et al., 1998). Thus, the difference in calculated irradiances is attributed to differences in model implementation, in particular that aerosols could not be varied in the web-based implementation of the FASTRT program. The Gregg and Carder model is a simple, two-stream model which consistently underestimated observed clear sky irradiance under GAP workshop conditions. This is notable in that it has been extensively used in past modeling analyses (e.g. Neale et al., 1998).
3. Intercomparison between measurements and models showed agreement between clear sky models, the SR18 spectral UV-B, and Macam broad band UV-A and UV-B sensors.
4. The broadband sensors provide good qualitative measures of UV exposure but the measurements cannot be used directly for quantitative dosimetry. The Macam sensors, though they are broad band sensors, do not measure UV-B and UV-A per se, instead they measure an irradiance weighted by their response function (Figure 1) which corresponds to about 40% and 50% of the total integrated solar UV-B and UV-A, respectively. This portion will of course depend on the spectral distribution of the incident irradiance and will, for example, vary with depth in the water. The effective response wavelength of the UV-B sensor in air is 320 nm, despite the fact that the maximum sensitivity of the sensor is at 310 nm, this will shift to longer wavelength at depth. The difference between the wavelength of maximum sensitivity and the effective wavelength under solar irradiance is caused by the much greater photon flux present at the long wavelength end of the solar UV-B band (Fig. 4). On the other hand, the UV-A spectrum is relatively "flat" so that the UV-A sensor measurements were equally correlated with model calculated irradiance at all wavelengths between 320 and 400 nm, despite the fact that the sensor has a peak response at 360 nm.

Probably the best use of the broadband data is to calibrate radiative transfer model calculations which can be done if the spectral responses of the sensors are well cha-

racterized as for the present study. To be useful in this regard, vigilance is needed in maintaining the sensors in calibration.

*Altitude effect on incident surface irradiance*

The Altitude Effect (AE) is defined as the increase in solar radiation with altitude, given as an increase in irradiance in per cent per 1000 m (Blumthaler et al. 1997). It is ideally measured by comparison of incident irradiance at low and high altitudes under the same conditions of other parameters influencing irradiance.

The two stations Piora and Kastanienbaum are separated by a mountain range and are thus too far apart to study the altitude effect per se (AE-abs) under ideal conditions. However, calculations were made of a relative altitude effect ($AE_{UV\text{-}A}$-rel, $AE_{UV\text{-}B}$-rel, normalized for PAR) under the ambient conditions at the two study sites to guide interpretation of the primary production data of the two Lakes Lucerne and Cadagno (Neale et al., 2001, this issue), in which the inhibitory influence of UV is investigated.

The assessments of incident surface radiation with the LiCOR and Macam broadband sensors at the two study sites during the GAP Workshop were used to investigate whether a positive altitude effect for UV-A and UV-B, relative to PAR (AE-rel), could be observed. The sensors used at Piora (1923 m a.s.l.) and Kastanienbaum (434 m a.s.l.) were intercalibrated before monitoring the two study sites. Since temporary breakdowns of the UV-A sensor at Piora prevented the collection of complete datasets (failure on 13 September), the campaign was repeated a year later during a similar period of the late summer season (from 1 until 6 September 2000) and confirmed the findings of the GAP Workshop (12 – 15 September 1999) presented below.

Incident surface PAR radiation (Fig. 2) at the two stations showed during the course of the days prevailingly sunny weather. The PAR-normalized data (UV-A / PAR and UV-B / PAR ratios) of the two stations were used to calculate for each time point of the day (in 10 min intervals) the ratios "Piora versus Kastanienbaum" which are shown in daily time courses (Fig. 6). Instantaneous AE can vary over a considerable range under cloudy conditions, as illustrated by the data of 12 September (in the early afternoon) and of 14 September. A ratio of AE-rel > 1 indicates a positive relative altitude effect (AE-rel), i.e. that the relative UV-A or UV-B irradiance at Piora is higher than at Kastanienbaum, when compared to PAR ($AE_{UV\text{-}A}$-rel, $AE_{UV\text{-}B}$-rel).

Figure 6 shows that during the assessed period the altitude effect (Piora versus Kastanienbaum) is variable during the course of a day and generally higher for UV-B than for UV-A, which is only slightly affected. This is in accordance with spectral assessments by Blumthaler et al. (1997) in the Swiss and Austrian Alps, where AE rose only slightly with shorter wavelength in the UV-A band and much more pronounced in the UV-B band. On average, AE is higher in the period before than after noon and even sinks often below a ratio of 1 in late afternoon (negative altitude effect). The early morning peaks, for which we do not have a straightforward explanation, are remarkable and were also consistently observed in the campaign of September 2000. It should be noted, however, that this altitude effect was measured in

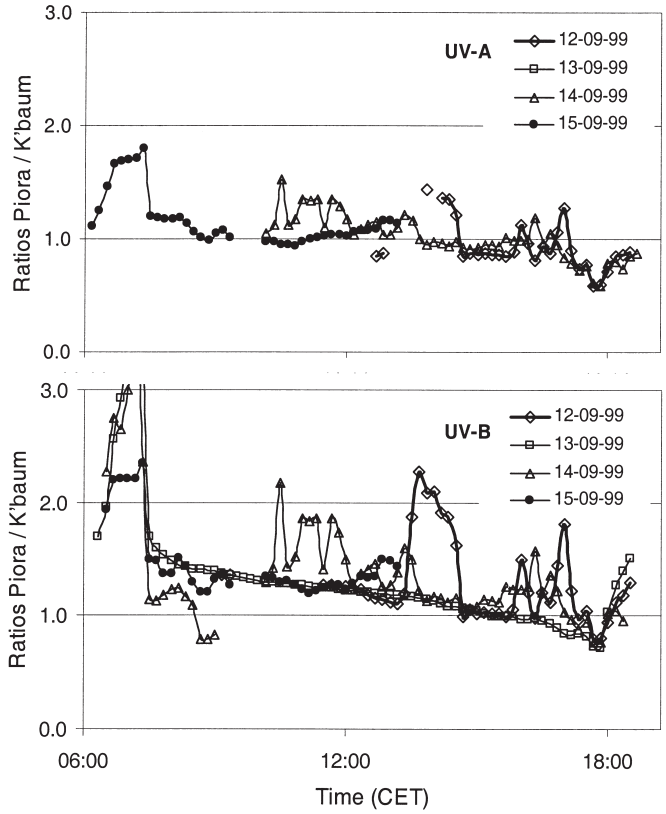


**Figure 6.** Altitude Effect (AE-rel) on incident surface irradiance of UV-A and UV-B, relative to PAR, calculated from data measured at Kastanienbaum (434 m a.s.l.) and at Piora (1921 m a.s.l.)

a mountainous environment and, hence, the portions of the sky seen by the sensors were different. This may affect the ratio of direct to diffuse irradiance at different times during the day.

Averages of PAR and UV-B radiation over the 1 h period around solar noon (12:30 h – 13:30 h, CET) are listed in Table 1, where the noon averages of the full period (12 – 15 September) are set against the noon averages of 13 September. This example illustrates how different recordings on a single day can be even on sunny days. Therefore the average of the full four days period should be a better indication of the real relationship between the sites. Irradiance at Piora was higher when it was clear, but because it was also cloudier it led to a lower overall incident PAR at Piora and roughly equal incident UVB at both sites.

### *Attenuation coefficients in Lakes Cadagno and Lucerne*

Depth profiles of $K_d$ for PAR, UV-A and UV-B, assessed on 12 September in Lake Cadagno and on 13 September in Lake Lucerne, revealed a depth dependence of

**Table 1.** Averages of PAR and UV-B radiation over the 1 h period around solar noon (12:30 h – 13:30 h, CET) at Piora (P, 1923 m a.s.l.) and Kastanienbaum (K, 434 m a.s.l) on 13 September 1999 and during the full period (12 – 15 Sep.)

| *Recorded at:* | Piora | | Kastanienbaum | | Ratios between the sites P and K | | |
|---|---|---|---|---|---|---|---|
| *Parameter:* | PAR µmol $m^{-2} sec^{-1}$ | UV-B µW $cm^{-2}$ | PAR µmol $m^{-2} sec^{-1}$ | UV-B µW $cm^{-2}$ | PAR P/K (PAR at P)/ (PAR at K) | UV-B P/K (UV-B at P)/ (UV-B at K) | $AE_{UV\text{-}B}$-rel (UV-B/PAR at P)/ (UV-B/PAR at K) |
| *Period:* | | | | | | | |
| full period | 1042 | 430 | 1289 | 415 | 0.81 | 1.04 | 1.28 |
| 13-Sep | 1331 | 523 | 1316 | 423 | 1.01 | 1.24 | 1.22 |

optical properties in both lakes particularly in the UV-B (Fig. 7A, B). $K_d$ PAR was quite constant with depth in Lake Lucerne and slightly lower than in Lake Cadagno, where $K_d$ increased considerably in the metalimnion (data not shown). The UV attenuation coefficients in Lucerne increased below 2.5 m which was the depth of surface mixed layer (Bossard et al., 2001, this issue). For $K_d(305)$ in Lucerne, the increase was more than 30% (Fig. 7A). A similar pattern of depth dependence was observed in $K_d$ calculated from the broadband UV measurements. Planktonic biomass was higher in the deeper stratified layer, however, this would primarily increase attenuation in the visible. This is consistent with an increase in the $K_d(443)$ (data not shown) observed between 5 and 8 m. However, because this layer of higher $K_d(443)$ occurred well below the increase in $K_d(305)$ it suggests that higher concentrations of chromophoric dissolved organic matter (CDOM) account for the higher UV attenuation in the lower layer. This CDOM being below the depth of 1% l surface UV-B irradiance would not be photobleached in contrast to CDOM in the surface layer (Morris and Hargreaves, 1997).

The overall $K_d$ for PAR and spectral UV over the upper 2.5 m of both lakes was calculated as this layer was the subject of intensive studies of photosynthesis in relation to UV exposure (see Callieri et al., 2001; Köhler et al., 2001; Neale et al., 2001; and Teubner et al., 2001; all in this issue). The spectral $K_d$ measured by the PUV-500 and Satlantic showed a characteristic exponential increase in attenuation with shorter wavelengths (Fig. 7C). The broadband attenuation coefficients measured using the Macam sensors (Bossard et al., 2001, this issue) are consistent with the spectral measurements of the PUV-500 and STOR-DAT, given the spectral range covered by each sensor (Fig. 7B). At all wavelengths $K_d$ was considerably larger in Lake Cadagno than in Lake Lucerne. Significant (>10% of surface UV-B) UV exposures to a near surface layer extended to about 1 m in L. Cadagno and to about 3 m in Lake Lucerne. For the comparison of phytoplankton response to UV between the lakes (see Neale et al., 2001, this issue), the depth at which irradiance at 320 nm is reduced to 50% of the surface was estimated. This depth was about 1 m in L. Lucerne and 0.3 m in L. Cadagno.

UV transparency is frequently quite limited in lakes due to the influx of CDOM from associated watersheds (Williamson et al., 1996). On this basis, both Lake Lucerne and Lake Cadagno are moderately UV transparent, with transparency to UV-B in the upper quartile of UV penetration compared to lakes of similar size

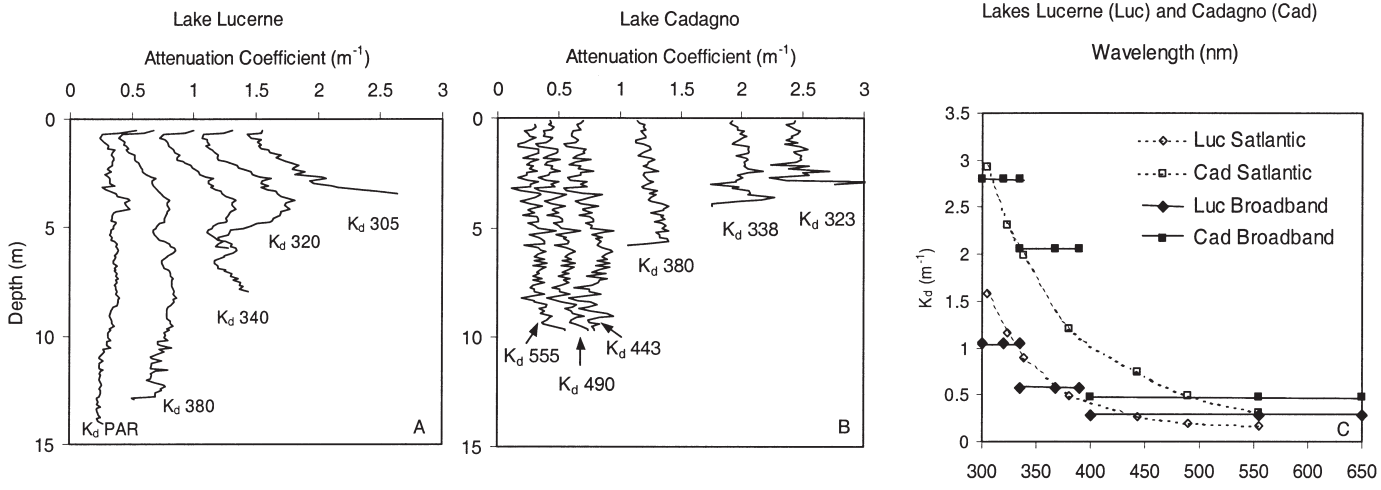


**Figure 7.** Attenuation coefficient for downwelling irradiance ($K_d$, $m^{-1}$)in Lakes Cadagno and Lucerne on 12/13 September 1999: (A) Depth profiles of the attenuation coefficient in Lake Lucerne using the PUV500 (PAR, and four wavelengths in the UV) (B) Depth profiles of the attenuation coefficient in Lake Cadagno using the STOR-DAT (six wavelengths in the UV and PAR) (C) Spectral attenuation coefficients as a function of wavelength for the uppermost 2.5 m. Coefficients are based on STOR-DAT measurements, except $K_d(305)$ is based on PUV500 measurements. Horizontal lines denote attenuation coefficients measured with the broadband sensors. The lines span the spectral region of greater than 50% response of each sensor relative to peak response (at wavelength of the middle symbol on the line segment). The line for the PAR sensor spans the 400–700 nm region (650–700 nm not shown)

(Williamson et al., 1996). The UV transparency of Lake Lucerne is in the same range as the N. American Great Lakes, such as Lake Erie (Smith et al., 1998). Lake Cadagno is not as clear as other alpine lakes (Montecino et al., 1997; Sommaruga and Psenner, 1997), but its moderate transparency is similar to other alpine lakes occupying a meadow catchment (Laurion et al., 2000).

## ACKNOWLEDGEMENTS

This study was carried out for the 7th International GAP Workshop, held on 9-17 Sept. 1999 in Zürich, Switzerland, and supported by the Swiss National Science Foundation (SNF), the Swiss Academies of Natural and Technical Sciences (SANW and SATW), the Swiss Society of Hydrology and Limnology (SGHL), by EAWAG, Zürich Water Supply and the University of Zürich, as well as by Hoffmann-La Roche, Lonza, Novartis, Canberra Packard S.A, Millipore AG and Faust Laborbedarf AG. We are grateful to John Morrow (Biospherical Instruments) for arranging the loan of the PUV-500 and operating the instrument during the GAP workshop, and to Margaret Squires for assistance in measuring irradiance profiles in Lake Cadagno.

## REFERENCES

Arrigo, K.R., 1994. Impact of ozone depletion on phytoplankton growth in the Southern Ocean: large-scale spatial and temporal variability. Marine Ecology Progress Series. 114: 1–12.

Blumthaler M. , W. Ambach and R. Ellinger, 1997. Increase of solar UV radiation with altitude. Journal of Photochemistry and Photobiology B: Biology. 39: 130–134.

Bossard P., S. Gammeter, C. Lehmann, F. Schanz, R. Bachofen, H.-R. Bürgi, D. Steiner and U. Zimmermann, 2001. Limnological description of the Lakes Zürich, Lucerne, and Cadagno. Aquat. Sci. 63/3: 225–249.

Callieri C., G. Morabito, Y. Huot, P.J. Neale and E. Litchman, 2001. Photosynthetic response of pico- and nanoplanktonic algae to UVB, UVA and PAR in a high mountain lake. Aquat. Sci. 63/3: 286–293.

Correll, D.L., C.O. Clark, B. Goldberg, V.R. Goodrich, D.R. Hayes Jr., W.H. Klein and W.D. Schecher, 1992. Spectral Ultraviolet-B radiation fluxes at the earth's surface: long-term variations at 39°N, 77°W. Journal of Geophysical Research. 97: 7579–7591.

Dahlback, A. and K. Stamnes, 1991. A new spherical model for computing the radiation field available for photolysis and heating at twilight. Planet. Space Sci. 39: 671–683.

Early, E., A. Thompson, C. Johnson, J. DeLuisi, P. Disterhoft, D. Wardle, E. Wu, W. Mou, Y. Sun, T. Lucas, T. Mestechkina, L. Harrison, J. Berndt and D. Hayes, 1998. The 1995 North American interagency intercomparison of ultraviolet monitoring spectroradiometers. J. Res. Natl. Inst. Stand. Technol. 103: 15-62.

Gregg, W.W. and K.L. Carder, 1990. A simple spectral solar irradiance model for cloudless maritime atmospheres. Limnology and Oceanography. 35: 1657-1675.

Koepke, P. and others, 1998. Comparison of models used for UV index calculations. Photochem. Photobiol. 67: 657-662.

Köhler, J., M. Schmitt, H. Krumbeck, M. Kapfer, E. Litchman and P.J. Neale, 2001. Effects of UV on carbon assimilation of phytoplankton in a mixed water column. Aquat. Sci 63: 294–309.

Laurion, I., M. Ventura, J. Catalan, R. Psenner and R. Sommaruga, 2000. Attenuation of ultraviolet radiation in mountain lakes: Factors controlling among- and within-lake variability. Limnol. Oceanogr. 45: 1274–1288.

Long, C.S., A.J. Miller, H.-T. Lee, J.D. Wild, R.C. Przywarty and D. Hufford, 1996. Ultraviolet Index forecasts issued by the National Weather Service. Bulletin American Meteorological Soc. 77: 729–748.

Montecino, V., G. Pizarro and G. Martínez, 1997. Optical climate (PAR and UV) and phytoplankton dynamics in a high mountain Andean lake (Laguna Negra, Chile). Verh. Internat. Verein. Limnol. 26: 441–445.

Morris, D.P. and B.R. Hargreaves, 1997. The role of photochemical degradation of dissolved organic carbon in regulating the UV transparency of three lakes on the Pocono Plateau. Limnol. Oceanogr. 42: 239–249.

Neale, P.J., R.F. Davis and J.J. Cullen, 1998. Interactive effects of ozone depletion and vertical mixing on photosynthesis of Antarctic phytoplankton. Nature. 392: 585–589.

Neale, P.J., E. Litchman, C. Sobrino, C. Callieri, G. Morabito, V. Montecino, Y. Huot, P. Bossard, C. Lehmann and D. Steiner, 2001. Quantifying the response of phytoplankton photosynthesis to ultraviolet radiation: Biological weighting functions versus *in situ* measurements in two Swiss lakes. Aquat. Sci 63/3: 265–285.

Ruggaber, A., R. Dlugi and T. Nakajima, 1994. Modeling of radiation quantities and photolysis frequencies in the troposphere. J. Atmos. Chem. 18: 171-210.

Smith, R.E.H., J.A. Furgal and D.R.S. Lean, 1998. The short-term effects of solar ultraviolet radiation on phytoplankton photosynthesis and photosynthate allocation under contrasting mixing regimes. J. Gt. Lakes Res. 24: 427–441.

Sommaruga, R. and R. Psenner, 1997. Ultraviolet radiation in a high mountain lake of the Austrian Alps: Air and underwater measurements. Photochem. Photobiol. 65: 957–963.

Teubner, K., A. Sarobe, M.R. Vadrucci and M.T. Dokulil, 2001. $^{14}C$ photosynthesis and pigment pattern of phytoplankton as size related adaptation strategies in alpine lakes. Aquat. Sci 63/3: 310–325.

Thompson, A., E.A. Early, J. Deluisi, P. Disterhoft, D. Wardle, J. Kerr, J. Rives, Y. Sun, T. Lucas, T. Mestechkina and P.J. Neale, 1997. The 1994 North American interagency intercomparison of Ultraviolet monitoring spectroradiometers. National Institute of Standards and Technology Journal of Research. 102: 279–322.

Williamson, C.E., R.S. Stemberger, D. P. Morris, T.M. Frost and S.G. Paulsen, 1996. Ultraviolet radiation in North American lakes: Attenuation estimates from DOC measurements and implications for plankton communities. Limnol. Oceanogr. 41: 1024–1034.

Received 12 June 2001;
revised manuscript accepted 18 July 2001.